

Numerical Simulations of Grassland Fire Behavior from the LANL - FIRETEC and NIST - WFDS Models

William E. Mell, Joseph J. Charney, Mary Ann Jenkins, Phil Cheney, Jim Gould

1. Introduction

Two physics-based computational fire models (FIRETEC and WFDS), capable of predicting time dependent fire behavior and fire-atmosphere interactions in three-dimensions are applied to wind driven grassland fires over flat terrain. Because these are surface fires (i.e., relatively little vertical flame spread) in a single, homogeneous fuel they are a good choice for the first stage in model evaluation. By “physics-based model” we mean that all modes of heat transfer (conduction, convection, radiation) present in both the fire-fuel and the fire-atmosphere interactions are modeled (in some approximation). These models are in their initial stages of development and validation. It is unlikely, due to their computational requirements, that they will replace present day operational models and approaches (e.g., McArthur meters, Nobel, 1980; BEHAVE, Andrews, 1986; Forest Service Fire Behavior Predictor, Hirsch, 1996; FARSITE, Finney, 1998) in the near future, at least in their present form. However, they do have the potential, in the near term, to provide reliable and detailed predictions of the behavior and effects of fire over a much wider range of conditions than operational models. Examples of near term research orientated applications include assessing the effect of fire on vegetation during prescribed burns, the response of a fire to a given fire break or thinning strategy, and furthering our understanding of the behavior and

March 5, 2008: To be published in "Remote Sensing and Modeling Applications to Wildland Fires" for Geosciences of Springer-Verlag and Tsinghua University Press

spread of fires through the intermix of structural and vegetative fuels that characterize the wildland-urban interface (WUI).

Fire models can be classified into three types (e.g., see Pastor et al., 2003): empirical, semi-empirical, or physics based (here we use “physical” and “physics based” interchangeably). Empirical models involve no physical modeling since they are based on statistical correlations of a given experimental data set. Semi-empirical models are based on energy conservation but do not distinguish between the different modes of heat transfer (conductive, convective, radiative). Physics-based models (such as FIRETEC and WFDS) attempt to solve (in some approximation) the equations governing fluid dynamics, combustion, and heat transfer. A complete, physics-based, wildland fire simulation must include approximations for the fire/atmosphere and the fire/fuel interactions

Section 2 provides an overview of the approaches used in the FIRETEC and WFDS models. Measurements from Australian (AU) grassland fire experiments can be used for model evaluation. These experiments are described in Section 3. WFDS predictions of the head fire spread rate and fire perimeters are compared to the AU grassland fire experiments in sections 4.1 to 4.3. To date similar comparisons have not been made with FIRETEC. For this reason, in Sec. 4.4 WFDS simulations were conducted of tall grass fires that match, as much as possible, the conditions of FIRETEC simulations reported in Linn and Cunningham (2005). This allowed a comparison of to be made of the two models. Finally, in Sec. 5 a summary of the findings is given.

2. Overview of the FIRETEC and WFDS Numerical Models

FIRETEC has been developed at Los Alamos National Laboratory (LANL) by Linn and colleagues (Linn 1997, Linn et al. 2002). FIRETEC provides fire spread predictions over landscape and requires significant computational resources (multiple processors). The governing model equations are based on ensemble averaging of the conservation equations for mass, momentum, energy, and chemical species. This results in additional closure equations which require a number of turbulence modeling assumptions. The numerical time stepping scheme explicitly handles the high frequency acoustic waves (Reisner, 2000). Chemical heat release from the combustion process occurs only in computational grid cells that contain the solid fuel (Linn et al., 2002). For grid cell

dimensions that are smaller than the flame length this is unrealistic and improvements are underway (Colman and Linn, 2003). Combustion is the result of a reaction rate that is a function of the density of both the solid fuel and the gas phase reactants, and an ad-hoc Gaussian-shaped probability density function (PDF) of the temperature. The use of this PDF is physically motivated but not yet validated. An assumed fraction of the heat produced by combustion is deposited in the solid fuel to help sustain pyrolysis. The solid fuel is assumed to be thermally thin. Thermal radiation transfer is computed using a diffusional transport approximation adapted from Stephens (1984). There is not, in the results reported to date, a model for the solid phase that handles pyrolysis which is coupled, through resolved heat fluxes, to a separate model for the gas phase which handles combustion. Instead, the pyrolysis of the solid phase and heat release from combustion in the gas phase are lumped together. This is the most significant difference (from a physical modeling point of view) between FIRETEC and other approaches, including WFDS.

WFDS is an extension of FDS (Fire Dynamics Simulator), a product of the National Institute of Standards and Technology (NIST) (McGrattan, 2004; McGrattan and Forney, 2004). The development of FDS started in the 1980's and it was created to simulate structural fires in a computationally efficient manner. It can be run on single processor desktop computers or on multiple processors and on a range of operating systems. FDS is currently used worldwide by 100s of fire protection engineers for structural fires and can be downloaded free. Smokeview, a companion software package, was also developed at NIST to interactively visualize FDS results (Forney and McGrattan, 2004). A survey of validation studies of FDS given in McGrattan (2004). The solution of the governing equations is based on basic Large Eddy Simulation concepts as first presented by Smagorinsky (1963). Recently, modifications to FDS were begun to handle fire spread through vegetative fuels (Rehm et al., 2003; Mell et al., 2007a) with the goal of simulating fire spread in an intermix of vegetative and structural fuels (i.e., WUI fires). This modified version of FDS is called WFDS and is used here to simulate grassland fires. Application of WFDS to elevated fuels has also begun (e.g., Mell et al., 2007c). A website, Mell et al. (2007b), provides information on the ongoing experimental and modeling work at NIST in wildland-urban interface fires. WFDS uses a low Mach number approximation to the governing equations developed by Rehm and Baum (1978). This approximation, which has been applied successfully to a wide range of fire and combustion problems, and the use of a fast direct solver for the pressure, results in computational speeds that are 10 to 100 times faster

than many other methods. The gas and vegetative phases are handled separately on different grids. The combustion model uses the well established mixture fraction based approach that assumes the fuel and oxygen react instantaneously over time scales characteristic of the flow (Bilger, 1980). The solid fuel is assumed to be thermally thin. Radiative and convective heat transfer within the fuel bed is directly modeled in manner similar to Albini (1985) and Morvan and Dupuy (2004). The pyrolysis model of Morvan and Dupuy (2004) is used. Char oxidation is not included. Thermal radiation transfer in the gas phase is computed with a finite volume based solver (Raithby and Chui, 1990). In the fuel bed a forward-reverse approximation (Ozisk, 1973; Mell and Lawson, 2001) is used for radiation transfer. Details on the model equations, numerical algorithm, and the approach used for igniting the solid fuel are given in Mell et al. (2007a), as are additional simulation results. Mell et al. (2007a) also provide a review of other physics-based models.

3. Overview of Grassland Fire Experiments

The experimental results and data used here were reported in Cheney et al. (1993) and Cheney and Gould (1995). The grassland fires were started by line fires, of varying lengths, along a fire break on the upwind edge of a grassland plot. One of two types of grass was present on a given plot: either *Eriachne burkittii* (kerosene grass) or *Themeda australis* (kangaroo grass). These two grasses differed in their structural and growth characteristics. In the models, however, physical differences in the fuel bed are accounted for only by the solid phase parameters listed in Table 1. The grassland plots measured 100 m x 100 m, 200 m x 200 m, or 200 m x 300 m and were surrounded by fuel breaks. At each corner of a plot the wind magnitude was measured every 5 s at a height of 2 m above the ground. Aerial photos and ground observations were used to obtain fire perimeters, head fire widths, and quasi-steady head fire spread rates. Figure 1a shows a photo of experiment F19 (see Sec. 4.3) and Figure 1b shows a snapshot from a WFDS prediction of the experiment.

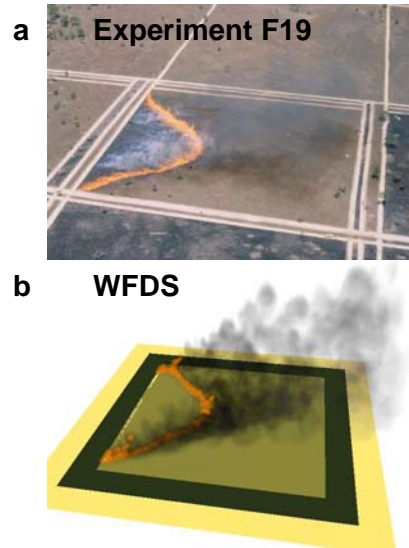


Figure 1. (a) Photograph of experimental fire F19 (see Sec. 4.3) at $t = 56$ s. (b) Snapshot of WFDS simulation of the same experimental fire at $t = 56$ s.

The following empirically based formula (Equation 4 in Cheney et al., 1998) relates the experimentally observed head fire spread rate R_0 (m/s), to the wind speed U_2 (m/s) at a 2 m height, the head fire width W (m), and the fuel moisture content M (%):

$$R_0 = (0.165 + 0.534 * U_2) * \exp[(-0.859 - 2.036 * U_2) / W] * \exp(-0.108 * M). \quad (1)$$

Cheney et al. (1998) defined the effective head fire width as the width of the fire, measured at right angles to the direction of head spread (and thus at right angles to direction of the wind at the head fire), which influenced the shape and size of the head fire during the next period of spread measurement (Cheney and Gould, 1995). The effective width of the head fire can also be defined as that portion of the perimeter where the flames are leaning towards unburnt fuel. In WFDS the head fire width was defined to be the distance between the flank fires one fire depth upwind of the trailing edge of the head fire. Figure 2 is a schematic showing, for an arbitrary fire perimeter, the head width, head-fire depth,

and ignition line fire. For a sufficiently large head fire width the observed spread rate, R_o , obtained its potential quasi-steady value, R_{ss} . This spread rate is obtained from Equation (1) for $W \rightarrow \infty$

$$R_{ss} = (0.165 + 0.534 * U_2) * \exp(-0.108 * M). \quad (2)$$

In this paper, simulated spread rates and head fire location from WFDS were compared to their experimentally observed values through the use of these empirical relations.

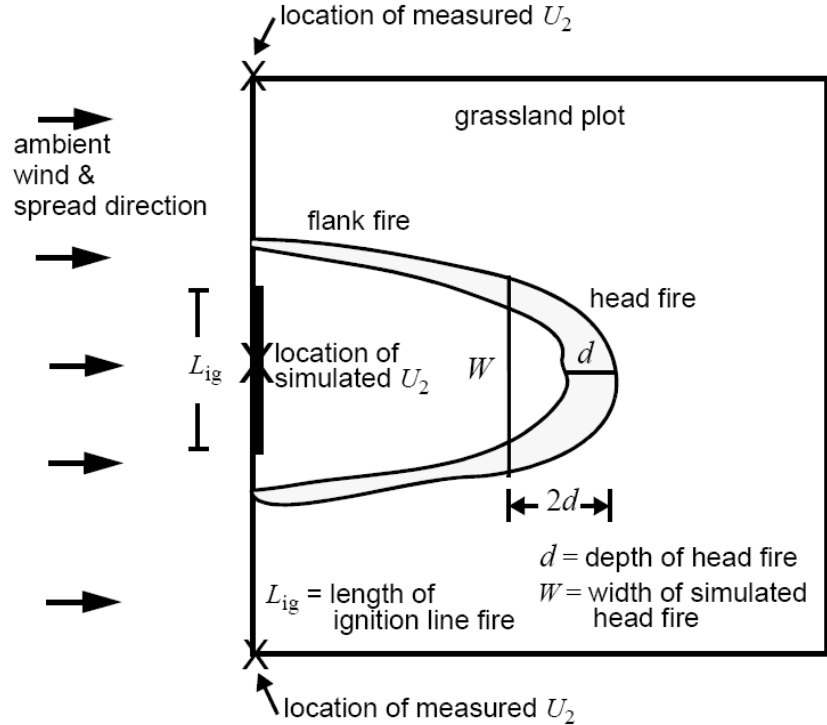


Figure 2. A schematic of a grassland fire. The ambient wind flows from left to right. The value of the wind speed, U_2 , in the experiments is obtained by averaging the magnitude of the horizontal velocity measured at a height of $z = 2$ m positioned at the upper and lower left-hand-side corners of the grassland plot. The value of the wind speed in the simulation is obtained from the computed component of the velocity vector parallel to the ambient wind at a height of approximately $z = 2$ m positioned above the center of the ignition line fire.

4. Approach and Results

This is the first comparison of FIRETEC and WFDS. As such, the primary objective is to assess how well the models predict experimentally observed trends of macroscopic behavior. FIRETEC simulations of the AU grassland experiments are not available at this time, so only comparisons of WFDS simulations and AU grassland fires appear here (see Sections 4.1 – 4.3). Comparisons between FIRETEC and WFDS were accomplished by running simulations of fire spread in the tall grass fuels reported by Linn and Cunningham (2005) (see Section 4.4). The authors feel it is important to compare both models against the AU grassland fire data in future experiments, and consider that such a comparison is a logical next step in the comparison of the models.

Table 1. Gas and solid properties used in the simulations

	Property	AU experiments		WFDS AU exp.	FIRETEC ^a tall grass	WFDS tall grass
		F19	C064			
Gas phase	heat of combustion of volatiles, kJ kg ⁻¹	n/a	n/a	15600	8914	15600
	radiation fraction	n/a	n/a	0.35	n/a	0.35
	soot fraction	n/a	n/a	0.02	n/a	0.02
Solid phase	surface area to-volume ratio, m ⁻¹	12240	9770	from exp	4000	4000
	char mass fraction	n/a	n/a	0.20	n/s	0.2
	grass height, m	0.51	0.21	from exp	0.7	0.7
	fuel element density, kg m ⁻³	n/a	n/a	512	n/a	512
	fuel loading, kg m ⁻²	0.313	0.283	from exp	0.7	0.7
	moisture, %	5.8	6.3	from exp	5.0	5.0

^aLinn and Cunningham (2005)

Table 1 lists the environmental parameters used in the simulations of fire in AU grasslands and tall grass. Parameters that were not measured in the AU experiments were determined from sources in the literature (Mell et al., 2007a). Two AU experiments, each with a different grass,

were considered. In Table 1, and in the following text, the two experiments are denoted F19 (natural *Themeda* grass) and C064 (cut, with cuttings removed, *Eriachne* grass).

4.1 Head Fire Spread Rate Dependence on Wind Speed in AU Grassland Fuel (WFDS only)

Four wind speeds, U_2 , were used in the simulations: $U_2 = 1, 3, 4, 5$ m/s. For each wind speed there were four different ignition line fires were used (a total of 16 cases) lengths: $L_{\text{ig}} = 8, 25, 50, 100$ m. Ignition lines with lengths of $L_{\text{ig}} = 8$ m and 25 m had a depth of 6.7 m; ignition lines $L_{\text{ig}} = 50$ m and 100 m had a depth of 3.3 m. The grassland fuel characteristics were those of experiment F19 in Table 1. The initial wind speed depends on height, z , above the ground according to a power law to approximate a boundary layer (Morvan and Dupuy, 2004):

$$u(x, y, z, t = 0) = U_{2,i} (z/2)^{1/7}. \quad (3)$$

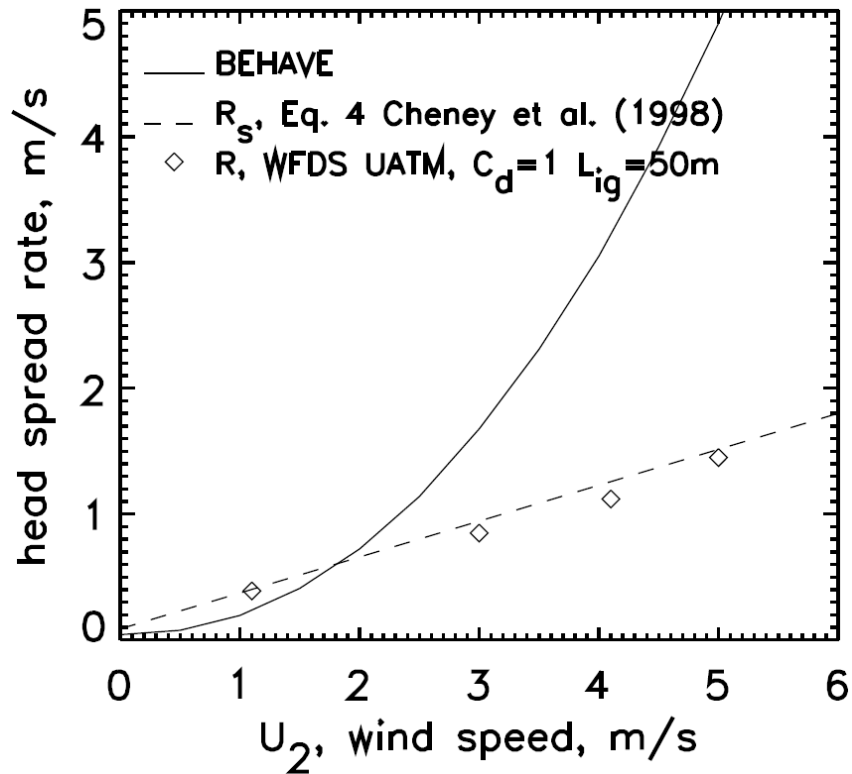


Figure 3. Spread rate versus wind speed from WFDS (symbols), BEHAVE (solid line) and Equation (2) (dashed line)

Here $U_{2,1}$ is the value in WFDS of the initial wind speed at a height of 2 m. As the simulation proceeds, the wind speed at this height is modified by the fire (due to both entrainment and blockage effects) and by drag from the grass. When comparing head fire spread rates from WFDS simulations and from Equation (1) a consistent value of U_2 must be used. In WFDS U_2 is the average value of the windward velocity, over the course of the simulation, in the first cell above the vegetation at the center of the ignition line-fire. The height of this velocity location is within $z = 1.95$ m - 2.1 m for the simulation cases reported here. Simulations with a number of grid resolutions and domain sizes were conducted to ensure that the results were not significantly influenced by grid resolution or boundary effects. All the WFDS simulations used an overall computational domain area of 1500 m x 1500 m with a 200 m x 200 m grassland plot in the center. The height of the computational domain was 200 m. The horizontal grid for a central 300 m x 300 m area containing the grassland

plot was $\Delta x = \Delta y = 1.66$ m; outside this central area $\Delta x = \Delta y = 3.33$ m. The vertical grid was stretched from $\Delta z = 1.4$ m to 5.5 m at a height of 200 m throughout the computational domain. Figure 3 is a plot of head fire spread rate versus wind speed. The physical parameters of the fuel are listed in Table 1. Spread rates from WFDS (symbols), BEHAVE (Andrews, 1986) (solid line) and Equation (2) (dashed line) are shown.

As will be seen below, in Figure 4, WFDS spread rates for $L_{ig} = 50$ m quickly reached a quasi-steady value. The linear dependence of the spread rate on the wind speed is well predicted by WFDS. The quantitative agreement of WFDS is also good, however it is important to note that the sensitivity of WFDS to realistic variations in environmental variables (wind speed, moisture content, etc.) has not yet been assessed. Another important issue is how the value of the wind speed, U_2 , is obtained. WFDS and both Equation (1) and Equation (2) use a value of U_2 that is the average wind speed at a height of approximately 2 m. This value of the wind speed was used to obtain BEHAVE results in Figure 3. However, in BEHAVE the default height of the wind speed is at the mid-flame height. Experimentally observed flame heights, for $U_2 = 5$ m/s, were 2.7 m for this fuel. This suggests that the wind speed input into BEHAVE should be larger, leading to a prediction of even faster spread rates than plotted in Figure 3. BEHAVE's over prediction of the spread rate for fuels with a surface-to-volume ratio of 13100 m^{-1} , which is a relatively fine fuel similar to the fuel used here, has been noted before, Gould (1988).

4.2 Head Fire Spread Rate Dependence on the Head Fire Width in AU Grassland Fuel (WFDS only)

Figure 4a below shows the fire spread rate versus the head fire width on the left from WFDS simulations with $U_2 = 1$ m/s and the four different

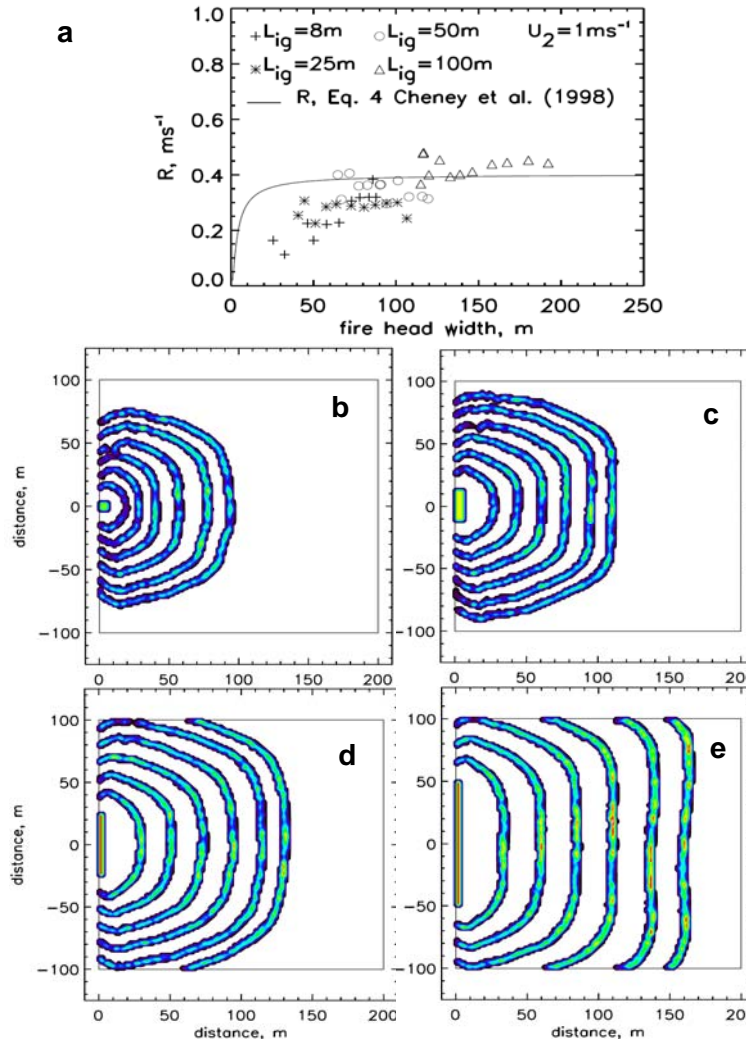


Figure 4. (a) Spread rate versus head fire width from WFDS for a wind speed of 1 m/s and four different ignition line fires is shown. The fire lines from which the spread data was determined shown on the right. The four ignition line lengths are (b) 8 m, (c) 25 m, (d) 50 m, (e) 100 m. The fire perimeters are plotted at times 0 s, 60 s, 120 s, 180 s, 240 s, 300 s, and 350 s. The fire spreads in a 200 m x 200 m grassland plot

lengths (Figures 4b-4e) of the ignition line fire. The solid line is the spread rate from Equation (1). The simulations reproduced the trend of an increasing head fire spread rate with an increasing width of the head fire. All L_{ig} cases reach a quasi-steady spread rate that is within 25 % of the

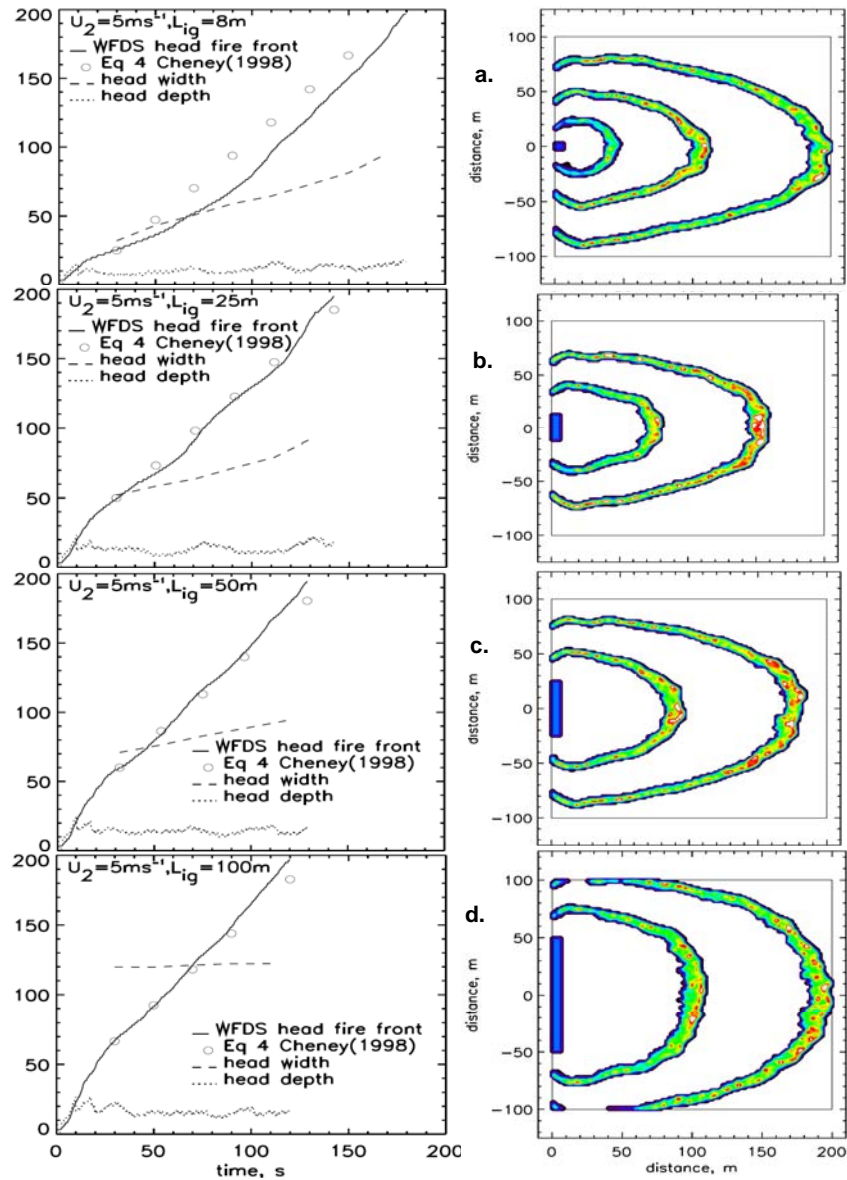


Figure 5. Left column shows the location of the leading edge of the head versus time from WFDS (solid line) and Equation 4 of Cheney et al. (1998) (circles) for a wind speed of 5 m/s and the four ignition line fires are used 8 m (a), 25 m (b), 50 m (c), and 100 m (d) long (same as Figure 4). The width (dashed line) and depth (dotted line) of the head fire are also plotted. The fire lines for each case are shown in the right column at 60 s intervals, starting at 0s

Equation (2) value. The experimental fires, as described by Equation (1), reached a quasi-steady spread rate at narrower head fires than the simulated fires. Figures 4b-4e are sequential snapshots of the burning region (shaded contours of the burning rate are shown) for each of the ignition line fire lengths used. Note that for the $L_{ig} = 50$ m and 100 m cases, Figures 4d and 4e respectively, the flank fires reach the upper and lower fire breaks.

In Figure 5 (left column) the location of the leading edge of the head fire versus time, from both WFDS (solid line) and from the Equation (1) (circles) with $U_2 = 5$ m/s, is shown in the left column. Each row in Figure 5 corresponds to a different L_{ig} . Also shown in the left column are the width (dashed line) and depth (dotted line) of the head fire. In each case an initial time period of relatively rapid spread is present, followed by a slower spread rate. This initial rapid spread may depend on the ignition procedure. This issue needs to be investigated. Equation (1) is implemented, using head fire widths from WFDS, to determine the location of the head fire (circle symbols) at the end of the initial time period of rapid spread. For the cases with $L_{ig} = 25$ m, 50 m, and 100 m WFDS predictions of the head fire location agree well with Equation (1). When $L_{ig} = 8$ m there is a period of time during which the head fire spread rate increases before reaching a quasi-steady value. The quasi-steady spread rate agrees well with Equation (1) at around $t = 110$ s (i.e., the solid line and a line through the circles become roughly parallel). The head width (dashed line) at which the simulated head fire spreads in a quasi-steady manner is approximately $W \geq 65$ m (note Figure 4a shows similar results for $U_2 = 1$ m/s). This is consistent with experimental observations that spread rates are relatively unaffected by L_{ig} when L_{ig} is sufficiently large. The head fire width is constant with time for $L_{ig} = 100$ m. Cheney and Gould (1995) noted at their highest wind interval between 4.7 and 7.1 m/s the head fire width of more than 125 m in open grassland is required to get spread rates within 10 percent of the quasi-steady rate of forward spread.

Figure 5 (right column) shows the fire perimeter at 60 s intervals. The relatively high wind speed results in head fire depths (10 m – 12 m) that are greater than the flank fire depths (5m – 7 m). This does not occur in the weak wind case ($U_2 = 1$ m/s in Fig. 4b-e). This behavior is consistent with field observations. Field measurements of the head fire depth for $L_{ig} = 175$ m and $U_2 = 4.9$ m/s range from 6.5 m to 10.5 m. Fire depths were interpreted from oblique photographs which were corrected and plotted onto a planar map of time isopleths of fire perimeter and fire depth.

4.3 Case Studies – Fire Perimeter in AU Grassland Fuel (WFDS only)

The mechanism of fire spread can change along the fire perimeter depending on the wind speed. In zero ambient wind, entrainment by the fire creates a local wind into which the entire fire line spreads (backing fire). In the presence of an ambient wind the downwind portion of the fire perimeter spreads with the wind (heading fire), the upwind portion of the fire perimeter spreads into the wind (backing fire), and the sides or flanks of the fire perimeter spread under conditions that can alternate between heading and backing fires. Note that in the cases considered here there are no backing fires since ignition occurred along the fire break at the upwind border of the plot. Backing fires, in which the flame tends to tilt away from the unburned fuel, can consume the fuel from the base upward, resulting in more complete fuel consumption. Heading fires, in which the flame tilts toward the unburned fuel, can be associated with lower fuel consumption because the grass ignites at the top and burns downward, covering the unburned fuel beneath with a protective coating of ash. The spread mechanism in flank fire can involve, depend on the fire/wind interaction, both the burning downward mechanism of head fires and the burning upward mechanism of backing fires. Thus, predicting the evolution of the entire fire line is much greater challenge, due to variation along the fire line of the fire/wind interaction and spread mechanisms, than predicting the behavior of just the head fire.

Neither FIRETEC nor WFDS can directly resolve the details in the grass fuel bed that differentiate a backing fire from a heading fire since the entire fuel bed is unresolved on the computational grid. For example, the height of the first grid cell in WFDS is 1.4 m while the height of the grass is 0.51 m. However, the fire/atmosphere interactions that occur over scales on the order of a few meters can be resolved. It is hoped that this level of resolution of the fire physics will be sufficient to capture the dynamics of the entire fire perimeter. It is important that a three-dimensional model predict the behavior of the entire fire perimeter. Otherwise, the overall heat release rate, fuel consumption, and smoke generation will be (to some degree) incorrectly predicted. These global fire characteristics are particularly important inputs to regional smoke transport models. In addition, the mechanisms behind extreme fire behavior (such as blow ups) are still poorly understood. A model that simulates the behavior of the entire fire perimeter, as opposed to only the head fire, is more likely to shed light on these issues.

In this section, model predictions of fire perimeters from two experimental cases are presented. In the first experiment, called F19, the

ignition line fire is 175 m long. This line fire was created with drip torches carried by two field workers walking for 56 s (87.5 m) in opposite directions from the center point to the ends the line fire. The average wind speed, measured at the corners of the 200 m x 200 m plot and not including measurements influenced by the fire, equaled 4.9 m/s. In the second experiment considered, called C064, the ignition line is 50 m long. The average wind speed was 4.6 m/s. Fuel bed characteristics are given in Table 1 for both experiments. Figure 6 shows the leading edge of the fire perimeter from the experiments (symbols) and the entire fire bed from WFDS (shaded contours of the burning rate) at three different times.

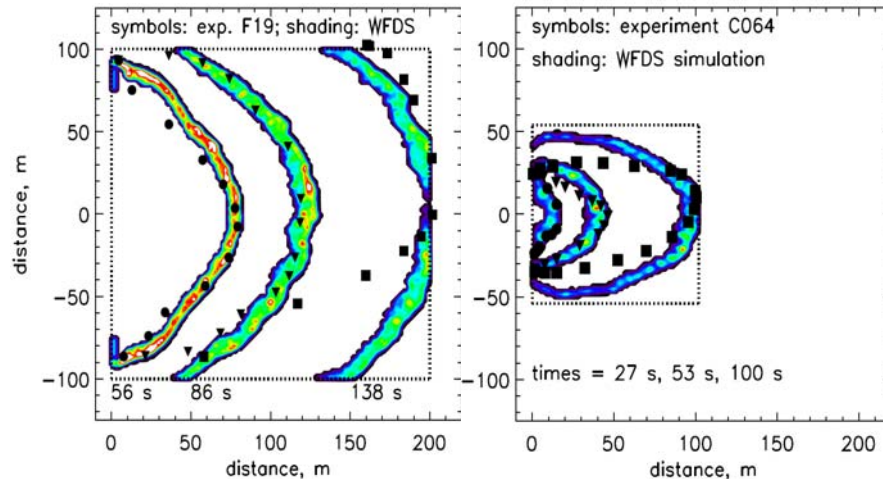


Figure 6. Fire perimeters from experiments (symbols) and WFDS simulations (shaded contours). Experiment F19 (left) and experiment C064 (right). See text for details and Table 1 for fuel/environmental parameters

Experiment F19 is shown in Figure 6 (left). A wind shift occurs in the experiment after $t = 86$ s which breaks the symmetry of the fire perimeter, this does not occur in WFDS since a constant wind orientation is assumed at the inflow boundary. As expected from the previous results, the spread of the head fire is well predicted at all times. Before the wind shift, the predicted fire perimeter closely matches the measured fire perimeter. After $t = 86$ s it's not clear how well WFDS performs because the wind shift significantly changes the observed fire perimeter. Also, long flanking fires (as, for example, those shown in Figure 5) do not develop for this case because the flank fires reach the fire breaks relatively quickly.

Experiment C064 is shown in Figure 6 (right). Extended flank fires do develop in this case. WFDS over predicts the spread rate of the flank

fires. The reasons for this are the subject of ongoing model development efforts. The current version of WFDS does not faithfully model the upward spread mechanism that can be present in flank fires. Instead, the fire burns downward through the grassland fuel bed everywhere along the perimeter. Also, in the field the depths of flank fires are significantly smaller than head fire depths for this experiment. The horizontal grid resolutions used here (1.66 m) adequately resolve the head fire depth but this may not be the case for the flank fires.

4.4 Simulation of Tall Grass (FIRETEC and WFDS)

Linn and Cunningham (2005) simulated fire spread in a fuel similar to the tall grass NFFL standard model 3. The parameters of this grass fuel are listed in Table 1. Two different lengths of an ignition fire line were used, $L_{ig} = 16$ m, 100 m and four different ambient wind speeds, constant with height, $U = 1, 3, 6, 12$ ms^{-1} . Six WFDS simulations were made: $U = 1, 3, 12$ for each of the two L_{ig} values. The results are listed in Table 2. The most significant difference in the two models was that backing fires (spreading upwind) and flank fires are more likely to occur, in a manner consistent with field observations, in WFDS. Figures 7a and 7b show plots of the fire perimeter at different times for $U = 3$ ms^{-1} and $L_{ig} = 16$ m and 100 m, respectively. Velocity vectors corresponding to the latest time, at a height of $z = 2$ m, overlaid the fire perimeters. Figures 8a and 8b are plots for a higher ambient wind speed of $U = 6$ ms^{-1} . Figures similar to Figures 7 and 8 here are provided by Linn and Cunningham (2005). Their Figures 3(a,b) and 4(a,b) correspond to Figures 7(a,b) and 8(a,b) here. Backing fires are clearly seen in the WFDS for the slower wind speed cases in Figure 7a and Figure 7b. Backing fires are also present in the faster wind speed cases of Figure 8a and Figure 8b. However, for the shorter ignition line case (Figure 8a) the backing fire was extinguished after $t = 50$ s due to diminished heat transfer to the upwind fuel.

For both FIRETEC and WFDS backing fires, when present, were more robust for the longer ignition lines. Field observations of backing fire behavior suggest that they are less likely to survive at higher wind speeds. This trend is not reproduced by FIRETEC, which was recognized by Linn and Cunningham (2005) and is under investigation. When a backing fire is not present in WFDS, as in case $L_{ig} = 16$ m, $U = 6$ ms^{-1} after $t = 50$ s, a similar head fire shape, which is necked inward toward the centerline, is predicted by both WFDS and FIRETEC. Head fire spread rates could not be compared because the presence of backing fires in WFDS influence the wind at the head fire locations

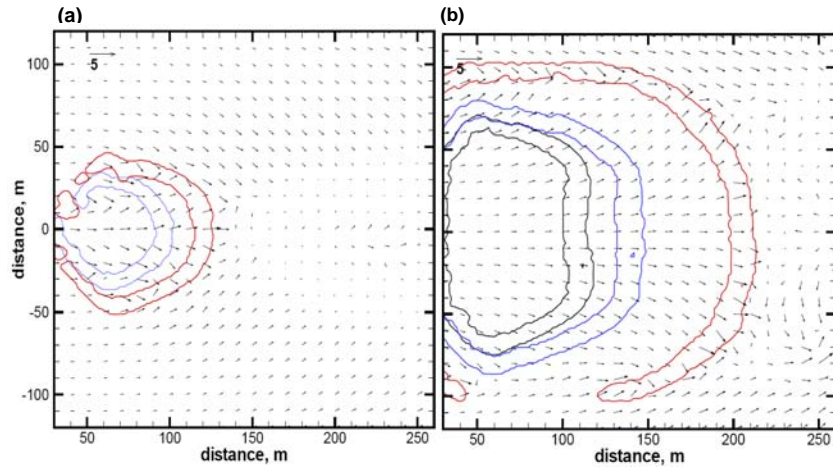


Figure 7. Fire perimeters (at different times) and velocity vectors (at a height of $z = 2$ m) for two different ignition line fire lengths and a constant ambient wind speed of $U = 3 \text{ ms}^{-1}$. Velocity vectors are from the same time as the latest fire perimeter. (a) Length of initial line fire is $L = 16$ m. Times of fire perimeters are $t = 150$ s, 250 s. (b) Length of initial line fire is $L = 100$ m. Times of fire perimeters are $t = 100$ s, 150 s, 250 s

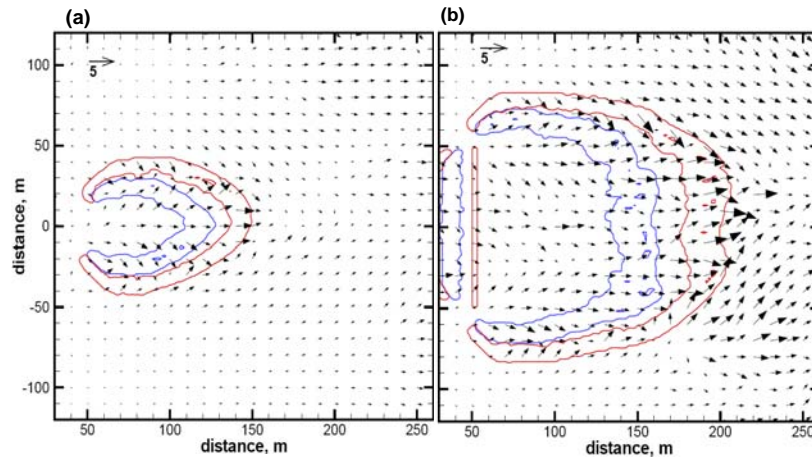


Figure 8. Fire perimeters (at different times) and velocity vectors (at a height of $z = 2$ m) for two different ignition line fire lengths and a constant ambient wind speed of $U = 6 \text{ ms}^{-1}$. Velocity vectors are from the same time as the latest fire perimeter. (a) Length of initial line fire is $L = 16$ m. Fire perimeters are at times $t = 90$ s, 150 s. (b) Length of initial line fire is $L = 100$ m. Fire perimeters are at times $t = 90$ s, 150 s

Table 2. Summary of results from FIRETEC and WFDS simulations of fire spread in tall grass

U	Lig	Backing fire		Flank fire	
		FIRETEC	WFDS	FIRETEC	WFDS
1	16	no	yes/no*	no	yes/no*
1	100	no	yes	no	yes
3	16	no	yes	yes	yes
3	100	no	yes	yes	yes
12	16	yes	yes/no**	yes	yes
12	100	yes	yes	yes	yes

* fire spread erratically and eventually extinguished due to the weak ambient wind

** backing fire survived for approximately 50 s before it was extinguished due to convective cooling.

5. Conclusions

Findings from Australian grassland experiments were used to evaluate the physics based fire model, WFDS. Whenever possible, fuel and atmospheric parameters measured in the experiments were used in the simulation. The spread rates of head fires were well predicted by WFDS. Spread rates of flank fires appear to be over predicted, but only one AU grassland experiment with freely spreading flank fires has been considered to date. Backing fires were not present in the experiments because ignition occurred just downwind of a fuel break. FIRETEC simulations for the AU grassland fuels were not available. However, WFDS simulations for fuels and conditions matching tall grass FIRETEC simulations (Linn and Cunningham, 2005) were run in order to compare results of the two models. Qualitatively the models produced similar results. The general trend, in observed grassland fires, of backing fires spreading more slowly as the ambient wind speed increased was not reproduced by FIRETEC. Both of these models are in their first stages of development and application to wildland fires. There is a great need for well documented full scale fires to aid further development in more complex fuel beds.

Acknowledgements

This work was sponsored in part by the USDA Forest Service Joint Venture Agreement 03-JV-11231300-088.

References

- Albini FA (1985) Wildland fire spread by radiation -- a model including fuel cooling by natural convection. *Combust. Sci. and Tech.* 45: 101-113
- Andrews PL (1986) BEHAVE: Fire behavior prediction and modeling system -- BURN subsystem part 1. USDA For. Serv. Gen. Tech. Rep. INT-194. See also <http://www.fire.org>
- Bilger RW (1970) Turbulent Reacting Flows. Ch. 4 in *Turbulent Flows with Nonpremixed Reactants*, Springer-Verlag
- Cheney NP, Gould JS, Catchpole WR (1993) The influence of fuel, weather and fire shape variables on fire spread in grasslands. *Int. J. Wildland Fire*, 3: 31-44
- Cheney NP, Gould JS (1995) Fire growth in grassland fuels. *J. Wildland Fire* 5: 237-347
- Cheney NP, Gould JS, Catchpole WR (1998) Prediction of fire spread in grasslands. *Int. J. Wildland Fire* 8: 1-13
- Colman JJ, Linn RR (2003) Non-local chemistry implementation in HIGRAD/FIRETEC. 2nd Intl. Wildland Fire Ecology and Fire Manage. Congress and 5th Symp. on Fire on Forest Meteorology, 16-20 November, Orlando, FL, American Meteorological Society
- Fons WL (1946) Analysis of fire spread in light forest fuels. *J. Agricultural Res.*, 72: 93-121
- Forney GP, McGrattan KB (2004) User's Guide for Smokeview Version 4: A Tool for Visualizing Fire Dynamics Simulation Data. NIST Special Publication 1017, <http://fire.nist.gov/bfrlpubs/>
- Finney MA (1998) FARSITE: Fire Area Simulator-Model, Development and Evaluation. USDA Forest Service, Rocky Mountain Research Station Paper, RMRS-RP-4
- Hirsch KG (1996) Canadian forest fire behavior prediction (FBP) system: user's guide. Canadian Forest Service, Special Report 7, Northwest Region, Northern Forestry Centre
- Larini M, Giroud F, Porterie B, Loraud J-C (1998) A multiphase formulation for fire propagation in heterogeneous combustible media. *Int. J. Heat Mass Transfer*, 41: 881-897
- Linn RR (1997) A transport model for prediction of wildfire behavior. Ph. D. thesis, New Mexico State University, also published as Los Alamos Report, LA-13334-T
- Linn R, Reisner J, Colman JJ, Winterkamp J (2002) Studying wildfire behavior using FIRETEC, *Int. J. Wildland Fire*, 11: 233-246
- Linn R, Cunningham P (2005) Numerical simulations of grass fires using a coupled atmosphere-fire model: Basic fire behavior and dependence on wind speed. *J. Geophysical Research*, 110
- McGrattan KB (2004) Fire Dynamics Simulator (Version 4), Technical Reference Guide. NISTIR Special Publication 1018, McGrattan K (ed), <http://fire.nist.gov/bfrlpubs/>

- McGrattan KG, Forney G (2004) Fire Dynamics Simulator (Version 4), Users Guide. NISTIR Special Publication 1019, <http://fire.nist.gov/bfrlpubs/>
- Mell WE, Lawson JR (2000) A Heat Transfer Model for Firefighters' Protective Clothing. *Fire Technology* 36: 39-68
- Mell W, Jenkins MA (2007a) A physics based approach to modeling grassland fires. *Int. J. Wildland Fire* 16: 1-22.
- Mell W, Rehm R, Maranghides A, Manzello S., Forney, G. (2007b) Wildland-Urban Interface and Wildland Fires. <http://www2.bfrl.nist.gov/userpages/wmell/public.html>
- Mell W, Maranghides A, McDermott R, Manzello S (2007c) Numerical simulation and experiments of burning Douglas fir trees. Submitted to *Combustion Theory and Modeling*.
- Morvan D, Dupuy JL (2004) Modeling the propagation of a wildfire through a Mediterranean shrub using a multiphase formulation. *Comb. Flame* 138: 199-210
- Nobel IR, Bary GAV, Gill AM (1980) McArthur's fire-danger meters expressed as equations. *Australian J. of Ecology* 5: 210-203
- Ozisk MN (1973) Radiative Heat Transfer and Interactions with Conduction and Convection. John Wiley & Sons, 1st Edition
- Pastor E, Zarate L, Planas E, Arnaldos J (2003) Mathematical models and calculations systems for the study of wildland fire behavior. *Prog. Energy. Combust. Sci.* 29: 139-153
- Rehm RG, Baum, HR (1978) The Equations of Motion for Thermally Driven, Buoyant Flows. *Journal of Research of the NBS* 83: 297-308
- Rehm R, Evans D, Mell W, Hostikka S, McGrattan K, Forney G, Bouldin C, Baker E (2003) Neighborhood-Scale Fire Spread. 5th Symposium on Fire and Forest Meteorology, November 16-20, American Meteorological Society, p J6.7
- Raithby GD, Chui EH (1990) A Finite-Volume Method for Predicting Radiant Heat Transfer in Enclosures with Participating Media. *J. Heat Transfer* 112: 415-423
- Reisner J, Wynne S, Margolin L, Linn R (2000) Coupled Atmosphere-Fire Modeling Employing the Method of Averages. *Monthly Weather Review* 128: 3683-3691
- Rothermel RC (1972) A mathematical model for predicting fire spread in wildland fuels. Research Paper INT-115, Intermountain Forest and Range Experiment Station, Odgen, Utah, USA
- Smagorinsky J (1963) General Circulation Experiments with the Primitive Equations I. The Basic Experiment. *Monthly Weather Review* 91: 99-164
- Stephens GL (1984) The parameterization of radiation for numerical weather prediction and climate models. *Monthly Weather Review* 112: 827-